[Short title + Author Name - P&H title] 17 (2024) 105480

Contents lists available at ScienceDirect

Arabian Journal of Chemistry

journal homepage: www.ksu.edu.sa

A potential antifungal agent: Insight into the antifungal mechanism against *Phomopsis sp*

Chunmei Yuan, Tao Zhang, Jiao Tian, Tianyu Deng, Hui Xin, Yi Liu, Yufang Zhang, Wei Xue *

National Key Laboratory of Green Pesticide, Key Laboratory of Green Pesticide and Agricultural Bioengineering, Ministry of Education, Center for R&D of Fine Chemicals of Guizhou University, Guiyang 550025, China

A R T I C L E I N F O

Keywords:
Myricetin
Thiazole
Antifungal activity
Mechanism of action research

A B S T R A C T

19 myricetin derivatives containing thiazole were designed and synthesized. Their fungicidal activities *in vitro* against ten species of plant pathogenic fungi were evaluated. Bioassay results indicated that some of compounds exhibited remarkable antifungal activities. Among them, **Z17** showed the strongest antifungal activity against *Phomopsis sp*, with *in vitro* EC_{50} of 12.3 μg/mL, which was superior to those of the control drug azoxystrobin (32.2 μg/mL) and fluopyram (77.7 μg/mL). In addition, **Z18** also had the inhibitory activity against the *Alternaria brassicae*, with an EC_{50} value of 32.5 μg/mL, which was much higher than azoxystrobin (49.3 μg/mL). **Z17** exhibited good protective activity (62.5 %) against *Phomopsis sp* on kiwifruit *in vivo* at 200 μg/mL. The results of *in vivo* experiments revealed that **Z18** could effectively defend against the infestation of cabbage by *Alternaria brassicae*, and improve the protection ability of the crop. Scanning electron microscopy (SEM) and fluorescence microscopy (FM) demonstrated that **Z17** could destroy the integrity of cell membrane of pathogen *Phomopsis sp*, thus affecting the normal growth of mycelia. The results of the mechanism research further confirmed that the action of **Z17** changed the mycelial morphology of *Phomopsis sp*, affected the permeability of cells, increased the leakage of cytoplasm and MDA contents. Molecular docking simulation results revealed that compound **Z17** could readily bind with the active site of SDH and could be a potential SDH inhibitor. In summary, this study provides new ideas for effectively controlling plant fungal diseases and developing new green chemical pesticide products.

1. Introduction

Plant pathogenic fungi seriously influence the flourishing development of world agriculture, posing a serious threat to global food security. At the same time, they also can endanger the normal development and growth of crops, resulting in reducing production and significant losses of fruits and vegetables. Some fungal toxins produced by plant pathogenic fungi can even endanger the health of humans and animals (Gao et al., 2023; Zhang et al., 2023a, 2023b). Kiwifruit is a popular fruit that contains many nutrients such as vitamins, polyphenols, and pectin (Figiel-Kroczyńska, 2021). Unfortunately, it is easy to be infected by pathogenic fungi such as *Phomopsis sp* after picking, resulting in fruit rot, leaf peel necrosis and other plant diseases, which leads to a decline in fruit quality and yield (Zhou et al., 2023). *Sclerotinia sclerotiorum* (*S. sclerotiorum*) and *Rhizoctonia solani* (*R. solani*) are extremely harmful to rape and rice, and the economic losses caused by these two pathogenic fungi are as high as 80 and 50 % each year (Dey et al., 2016; Liu et al., 2022). Cruciferous vegetables are rich in nutrients and good for human health. Eating more cruciferous vegetables can prevent the occurrence of cancer (Zeng et al., 2023). *Alternaria brassicae* (*A. brassicae)* is one of the most common and destructive fungal diseases in cruciferous family, and spreads in different places mainly through seed transmission and harms the leaves and the whole plant, which leads to a serious decline in the quality and quantity of cabbage (Belmas et al., 2018). At present, traditional chemical fungicides, including benzimidazoles, dithiocarbamates, SDH inhibitors, and azoles, are still the most commonly used methods for controlling various plant pathogens due to their high efficiency, broad spectrum, economy, and ease of access. However, with the extensive and long-term application of fungicides, an increasing number of pathogens have accelerated the emergence and development of drug resistance, causing serious environmental problems. This greatly reduces the effectiveness of fungicides

Peer review under responsibility of King Saud University.
* Corresponding author.
E-mail address: wxue@gzu.edu.cn (W. Xue).

https://doi.org/10.1016/j.arabjc.2023.105480
Received 21 September 2023; Accepted 22 November 2023
Available online 23 November 2023

and requires an increase in dosage during application process, leading to a vicious cycle (Gao et al., 2023). Therefore, it is urgent to discover and create efficient and low toxic green antifungal drugs by using natural products as the framework for structural modification.

At present, the application of natural products for drug molecular design in agriculture has become one of the hotspots. Myricetin is a natural polyhydroxy flavonoid compound that can be extracted from many plants, fruits, vegetables, and beverages, such as bayberry bark, tomatoes, onions, red wine and so on (Ong and Khoo, 1997). In the early research work of our group, it was found that myricetin and its derivatives had a wide range of biological activities, such as antiviral (Tang et al., 2020), antibacterial (Rashed et al., 2014; Liu et al., 2021), and anticancer (Xue et al., 2015). For example, Peng et al. designed and synthesized a series of myricetin derivatives containing 1,3,4-oxadiazole sulfide, which showed good antiviral activity. Compound **A** (Fig. 1) showed obvious curative and protective effects against tobacco mosaic virus, with EC_{50} values of 195.2 ± 4.4, 189.9 ± 3.5 μg/mL, which was superior to that of ningnanmycin (296.4 ± 3.8, 307.6 ± 4.4 μg/mL) (Peng et al., 2021). Jiang et al. introduced the active groups piperidine and dithiocarbamate into myricetin. **B** (Fig. 1) exhibited the excellent antibacterial activity against *Xac* (*Xanthomonas axonopodis pv. citri*), with EC_{50} value of 0.1 μg/mL, which was better than that of thiazoin (60.0 μg/mL) (Jiang et al., 2020). Cao et al. constructed a series of myricetin derivatives containing isoxazole, among which **C** (Fig. 1) demonstrated good activity against *S. sclerotiorum*, with EC_{50} value of 13.2 μg/mL, which was higher than that of the control agent azoxystrobin 23.0 μg/mL (Cao et al., 2023). Liu et al. introduced a myricetin derivative containing pyrazol piperazine amide, and **D** (Fig. 1) had an EC_{50} of 16.9 μg/mL against *Phomopsis sp*, which was better than that of azoxystrobin 50.7 μg/mL (Liu et al., 2023). Therefore, myricetin was expected to be used as the lead compound in this study to obtain some novel compounds with higher antifungal activity.

Thiazole rings containing two heteroatoms N and S are a good pharmacodynamic molecule and are widely found in natural products (Rouf and Tanyeli, 2015). It has been widely used due to its antibacterial (Zhu et al., 2021), anticancer (Cai et al., 2016), insecticidal (Borcea et al., 2021), anti-inflammatory (Kamat et al., 2020), antiviral properties (KanagasAbapathy et al., 2023), and high bioavailability and good biocompatibility (Meng et al., 2022). For example, commercially available fungicide isothiazolinone (Silva et al., 2020), antifungal agent abafungin (Borelli et al., 2008), insecticide thiamethoxam (Ferreira-Junior et al., 2018) and the anti-cancer drug dasatinib (Bolf et al., 2023) all contain thiazole ring structures (Fig. 2). Therefore, the innovation of thiazole structure and its extensive biological activity have attracted widespread attention from pharmaceutical chemists.

On the basis of these considerations, we assumed to introduce thiazole functional groups into the structure of myricetin through active splicing, and a series of myricetin derivatives containing thiazole structures were designed and synthesized (Fig. 3). Subsequently, the antifungal activity of the target compounds were evaluated and screened. Through antifungal activity screening and studying the mechanism of action, we found out the compound **Z17** with broad-spectrum antifungal activity, which provided sufficient support for further development of myricetin derivatives.

2. Materials and methods

2.1. Instruments and chemicals

The measurement of melting points was carried out using an XT-4 binocular microscope without calibration (Beijing, China). The relevant information for NMR was obtained by using a 500 MHz nuclear magnetic resonance instrument (JEOL-ECX500, Japan Electronics Co., Tokyo, Japan). High-resolution mass spectrometry (HRMS) used the Thermo Scientific Q Active mass spectrometer (Missouri, USA). SEM data obtained from FEI Nova Nano 450 (Oregon, USA). Observing the staining of cell hyphae using Olympus BX53 fluorescence microscope (Tokyo, Japan). The permeability of cell membranes was measured using a conductivity meter Leici DDSJ-3O8F (Shanghai, China). The content of MDA was determined by the Multiskan FC microplate reader assay (Shanghai, China). The release of cell contents was recorded by an N-5000 ultraviolet spectrophotometer (Shanghai, China). All reagents and solvents used in the experiment were purchased from Shanghai Titan Chemical Co., Ltd. (Shanghai, China) and Beijing Solarbio Technology Co., Ltd. (Beijing, China). All reagents are analytically pure and can be used directly.

2.2. Synthesis

2.2.1. Synthesis of intermediates *1*–*5*

Intermediates **1** and **2** were synthesized by referring to the literature (Chen et al., 2019). The intermediates **3** to **5** were prepared according to the methods reported in the literature and slightly modified (Das et al., 2006; Zhou et al., 2022; Zhang et al., 2023a, 2023b). Firstly, 5.73 mmol

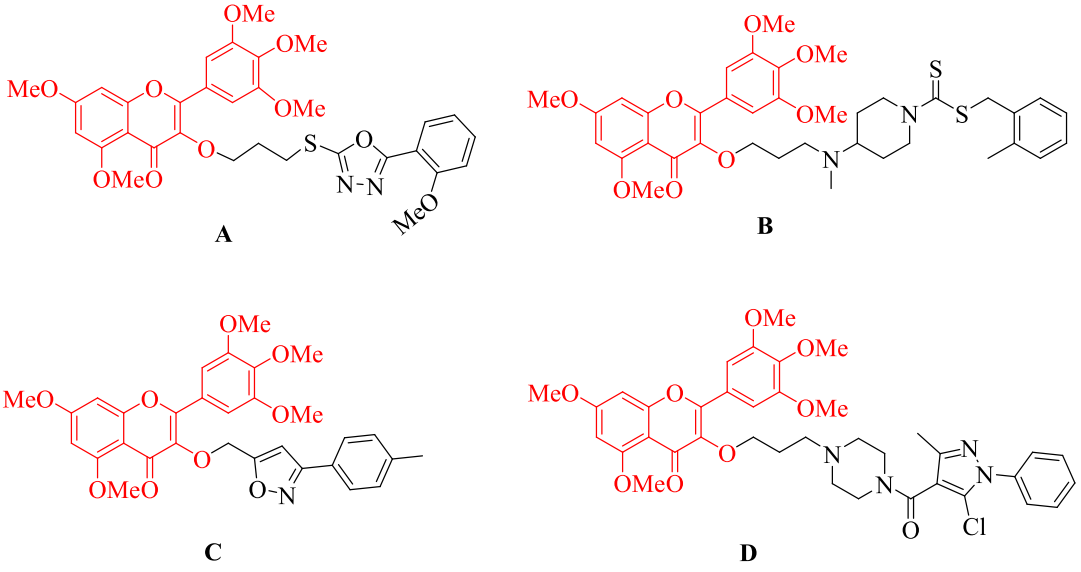

Fig. 1. Structures of myricetin derivatives previously reported by our group.

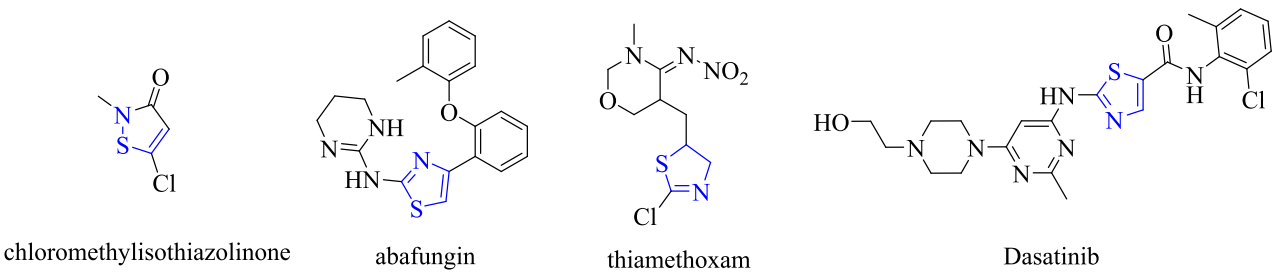

Fig. 2. Thiazole active group fragment.

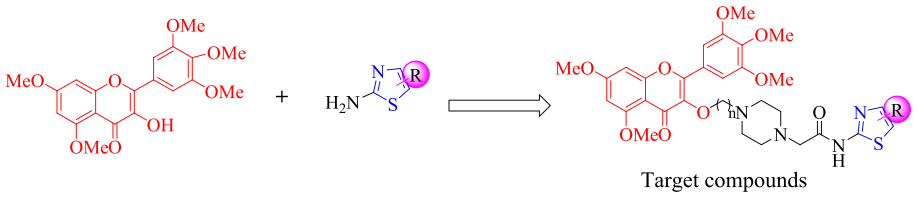

Fig. 3. The design ideas of target compounds.

4-*tert*-butoxypiperazine, 5.73 mmol K_2CO_3, and 9.98 mL acetonitrile solvent were added to the round-bottom flask, heated at 80 ℃ for 0.5 h, and then adding intermediate **2**. The reaction was monitored by TLC (dichloromethane:methanol = 30:1). After the reaction was completed, the reaction system was poured into ice water and white solid was precipitated to obtain intermediate **3**. With methanol as the solvent, intermediate **3** (1.59 mmol) was added into a 100 mL round-bottomed flask, stirring at 80 ℃ for 10 min, then slowly adding 0.59 mL of HCl to the reaction vessel using a pipette, and continue refluxing for 2 h to gain intermediate **4**. The different substitutions of 2-aminothiazole (8.76 mmol), 0.92 mL pyridine and 9.15 mL acetonitrile were successively added into the round-bottom flask and stirred at room temperature for 0.5 h, after adding 0.84 mL chloroacetyl chloride under the condition of ice bath. At the end of the reaction, the intermediate **5** was obtained by vacuum concentration and filtration.

2.2.2. *Synthesis of target compounds **Z1-Z19***

The synthetic steps of the target compounds **Z1-Z19** referred to the methods reported in the literature (He et al., 2020; Peng et al., 2023). 6.75 mL DMF was used as solvent, 3.54 mmol K_2CO_3 as acid binder, 0.88 mmol intermediate **4** was added to a round-bottom flask, stirred at room temperature for 45 min until solid dissolution, and then 1.77 mmol intermediate **5** was added to the reaction system and heated at 80 ℃ for 12 h. After the reaction was complete, the system was poured into ice water. The oil was extracted by dichloromethane and dried with anhydrous Na_2SO_4, then concentrated under reduced pressure. The obtained oil was further purified by column chromatography (ethyl acetate: methanol = 30:1 *v/v*).

2.3. *Antifungal activity assay in vitro*

The inhibitory effect of **Z1-Z19** on fungi *in vitro* was tested with mycelium growth rate method (Fang et al., 2022). In addition, compounds with better activity were selected for further determination of the half effective concentration (EC_{50}). The commercial agents azoxystrobin and fluopyram were used as positive controls. Each experiment was repeated three times.

2.4. *Antifungal bioassay in vivo*

According to the methods reported in the literature (Zhou et al., 2023), the inhibitory activity of **Z17** against *Phomopsis sp* on kiwifruit was evaluated at 200 and 100 μg/mL with azoxystrobin as the positive control. The effect of **Z18** against *A. brassicae* on cabbage was evaluated by using the azoxystrobin as positive control, and the disease degree was graded as follows. There is grade 0, there is no disease. At grade 1, the lesion area accounted for less than 5 % of the leaf area. At grade 2, the lesion area accounted for 6–10 % of the leaf area. At grade 3, the lesion area accounted for 11–25 % of the leaf area. At grade 4, the lesion area accounted for 26–50 % of the leaf area. At grade 5, the lesion area accounted for more than 50 % of the leaf area, with azoxystrobin as the positive control (He et al., 2021; Zhang et al., 2022). Each experiment was repeated three times.

2.5. *Scanning electron microscope and fluorescence microscope*

With reference to the previous literature (Fang et al., 2022; Xie et al., 2022), **Z17** was tested by scanning electron microscope and fluorescence microscope to observe the morphological changes of mycelia, with the aim of studying the inhibitory effect of **Z17** on *Phomopsis sp* further.

2.6. *Formation of sclerotia*

The experiment of **Z17** on sclerotia formation was performed by previously reported in the literature (Zhang et al., 2018).

2.7. *Permeability of cell membranes*

According to previous reports, the permeability of cell membranes was analyzed by measuring the relative conductivity of mycelium (Wang et al., 2020).

2.8. *Release of cellular contents*

Ultraviolet spectrophotometer was used to measure the absorbance of the supernatant at 260 and 280 nm, respectively, thereby to judge the degree of cytoplasmic release (Cao et al., 2023).

2.9. *Determination of malondialdehyde content*

The content of malondialdehyde (MDA) reflects the degree of lipid peroxidation of animal and plant cell membranes. The higher the content of MDA is, the higher the degree of lipid peroxidation of cell membranes is, and the more serious the damage to cell membranes is. According to the methods reported in the literature, the content of MDA in **Z17** was studied (Chen et al., 2023; Hu et al., 2023).

2.10. Molecular docking

To further investigate whether SDH is a potential target for action, we conducted molecular docking of **Z17** and fluopyram (Succinate dehydrogenase inhibitor) with SDH (Liu, et al., 2023). Discovery studio 2019 tools and PyMOL Win software were used to simulate and verify the binding ability of **Z17** to SDH active proteins (PDB: 2FBW).

3. Results and discussion

3.1. Chemistry

The **Z1-Z19** were synthesized according to the designed route of Scheme 1. All the compounds were characterized by NMR and HRMS, the detailed data are in the Supporting material.

3.2. In vitro antifungal activity

Z1-Z19 were tested for *in vitro* inhibitory activities against 10 plant fungi at 100 μg/mL. The test results were shown in Table 1 that **Z17** had a certain inhibitory activity on all the test strains. **Z17** possessed the best inhibitory effect on *Phomopsis sp*, with an inhibition rate of 94.3 %, which was significantly higher than those of the azoxystrobin (65.2 %) and fluopyram (51.9 %). Besides, **Z17** also exhibited good inhibitory effects on *R. solani*, *S. sclerotiorum*, *Fusarium graminearum*, *Botrytis cinerea*, and *A. brassicae*, with inhibition rates of 80.3, 83.3, 69.5, 75.8, and 69.0 %, respectively, which were superior to those of azoxystrobin 74.5, 62.4, 60.9, 68.8, and 59.5 %. At the same time, **Z6** also had good inhibitory effects on *S. sclerotiorum* and *Phomopsis sp*, with inhibition rates of 80.8 and 91.7 %, which were better than the those of azoxystrobin 62.4 and 65.2 %. The inhibition rates of **Z4** on *Phomopsis sp* and *Phytophthora capsici* were 70.4 and 80.2 %, which were better than the those of azoxystrobin 65.2 and 71.2 %. The inhibitory rate of **Z18** on *A. brassicae* was 72.0 %, which was higher than the control drug azoxystrobin 59.5 %.

As shown in Table 1, we could see that the introduction of a thiazole moiety with antifungal activity into myricetin can significantly enhance its inhibitory effect. Therefore, we studied the control effects of different substituents on plant pathogens by changing the structure of thiazole and analyzed their structure–activity relationships. When the R = 4-C$(CH_3)_3$ and R = 4-Ph substituents, their *in vitro* antifungal activities were better than that of R = 5-Br and R = 4-F-Ph, such as **Z17** (n = 3, R = 4-C$(CH_3)_3$) > **Z6** (n = 3, R = 5-Br), **Z9** (n = 3, R = 4-Ph) > **Z16** (n = 4, R = 4-F-Ph). This indicates that when the R group was an electron donating group, myricetin derivatives have better antifungal activities. In addition, we have found that brominated alkanes with a carbon atom number of 3 have better antifungal activity than those with a carbon atom number of 4, such as (**Z17**, n = 3, R = 4-C$(CH_3)_3$ > (**Z18**, n = 4, R = 4-C$(CH_3)_3$), (**Z11**, n = 3, R = 4-Cl-Ph) > (**Z12**, n = 4, R = 4-Cl-Ph), which indicated that shortening the carbon chain can make the binding between compounds closer and have better antifungal effects.

In summary, when the number of C atoms in brominated alkanes was 3 and the R group on the thiazole group was an electron donating group, the antifungal activities increase significantly. In order to further verify the antifungal efficacy, EC_{50} test was conducted on some compounds. As shown Fig. 4 and Table 2, **Z17** had the optimal EC_{50} value for *Phomopsis sp* (12.3 μg/mL), which was superior to those of azoxystrobin (32.2 μg/mL) and fluopyram (77.7 μg/mL). The EC_{50} value of **Z18** against *A. brassicae* was 32.5 μg/mL, which was better than the that of azoxystrobin (49.3 μg/mL).

3.3. Z17 in vivo fungicidal activities resist Phomopsis sp

The results of *in vivo* experiments showed that **Z17** had good protective and curative effects (Fig. 5, Table 3) on kiwifruit infected with *Phomopsis sp* at 200 μg/mL. The protective effect of **Z17** was 62.5 % on

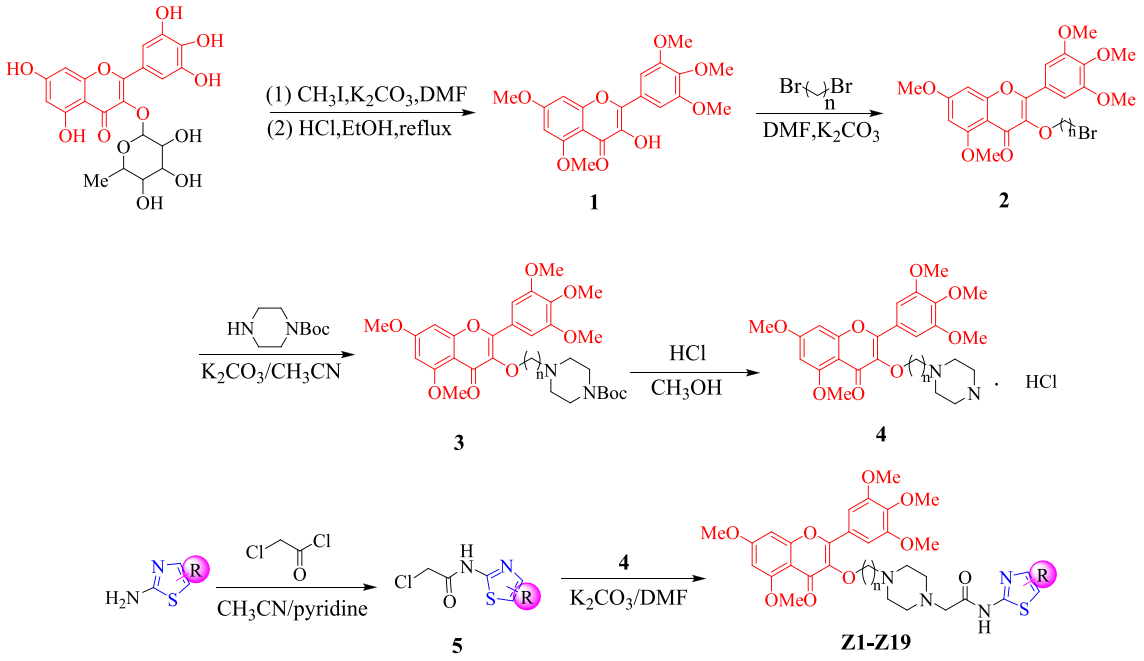

Z1:n=3,R=H **Z2**:n=4,R=H **Z3**:n=3,R=5-CH_3 **Z4**:n=4,R=5-CH_3
Z5:n=4,R=5-NO_2 **Z6**:n=3,R=5-Br **Z7**:n=3,R=4-CH_3 **Z8**:n=4,R=4-CH_3
Z9:n=3,R=4-Ph **Z10**:n=4,R=4-Ph **Z11**:n=3,R=4-Cl-Ph **Z12**:n=4,R=4-Cl-Ph
Z13:n=3,R=3,4-di-Cl-Ph **Z14**:n=4,R=3,4-di-Cl-Ph **Z15**:n=3,R=4-F-Ph **Z16**:n=4,R=4-F-Ph
Z17:n=3,R=4-tert butyl **Z18**:n=4,R=4-tert butyl **Z19**:n=3,R=4,5-di-CH_3

Scheme 1. Synthetic route of compounds **Z1-Z19.**

Table 1
In vitro antifungal activities of **Z1–Z19** at 100 μg/mL.

Compounds	Inhibition rates (%) [a]									
	Ps	*Ss*	*Bd*	*Rs*	*Fg*	*Pc*	*Bc*	*Ab*	*Cg*	*Fo*
Z1	47.4 ± 0.9	41.6 ± 2.9	22.7 ± 2.2	58.6 ± 1.9	34.8 ± 1.9	63.9 ± 1.4	59.2 ± 2.7	36.2 ± 2.4	22.7 ± 2.2	18.7 ± 3.4
Z2	66.5 ± 0.9	59.6 ± 2.3	29.3 ± 2.3	58.2 ± 2.3	30.9 ± 2.7	59.7 ± 1.2	61.3 ± 1.2	33.2 ± 2.3	29.3 ± 2.3	21.8 ± 1.6
Z3	49.6 ± 2.4	60.8 ± 2.4	24.8 ± 1.8	54.0 ± 3.0	33.9 ± 1.9	73.8 ± 1.7	60.0 ± 2.0	33.6 ± 4.3	24.8 ± 1.8	19.8 ± 7.2
Z4	70.4 ± 1.2	66.5 ± 1.8	33.1 ± 2.6	57.7 ± 1.7	36.5 ± 3.7	80.2 ± 2.4	65.8 ± 2.3	41.4 ± 1.2	33.1 ± 2.6	19.8 ± 4.8
Z5	28.3 ± 3.5	5.3 ± 3.8	13.2 ± 1.4	54.8 ± 2.0	16.7 ± 4.2	30.5 ± 2.9	50.8 ± 1.1	22.4 ± 2.0	13.2 ± 1.4	7.1 ± 5.0
Z6	91.7 ± 1.7	80.8 ± 1.6	26.4 ± 2.3	63.2 ± 1.8	43.8 ± 1.7	57.5 ± 1.2	65.8 ± 1.1	62.1 ± 3.1	26.4 ± 2.3	30.6 ± 6.5
Z7	65.7 ± 0.9	60.0 ± 3.3	19.8 ± 2.7	49.8 ± 1.4	37.3 ± 1.9	58.4 ± 0.9	51.7 ± 5.0	37.1 ± 1.9	19.8 ± 2.7	26.6 ± 1.6
Z8	73.5 ± 0.9	62.0 ± 2.3	26.4 ± 2.3	45.2 ± 2.2	37.8 ± 1.7	60.9 ± 3.4	52.1 ± 2.2	37.5 ± 1.7	26.4 ± 2.3	27.0 ± 1.7
Z9	53.5 ± 2.7	60.8 ± 2.0	24.8 ± 1.1	39.7 ± 2.0	27.5 ± 3.7	37.8 ± 3.4	62.1 ± 0.9	37.1 ± 2.8	24.8 ± 1.1	26.2 ± 3.3
Z10	69.1 ± 3.7	62.4 ± 1.1	23.6 ± 0.9	45.2 ± 0.9	32.2 ± 1.9	38.6 ± 0.9	65.0 ± 2.8	49.1 ± 1.2	23.6 ± 0.9	16.3 ± 5.9
Z11	53.9 ± 3.5	64.9 ± 2.6	18.6 ± 1.7	51.5 ± 4.4	38.6 ± 1.7	56.2 ± 1.4	66.7 ± 2.3	35.3 ± 1.4	18.6 ± 1.7	24.6 ± 5.5
Z12	34.3 ± 1.7	45.7 ± 1.6	24.8 ± 1.1	49.8 ± 1.4	38.2 ± 2.9	30.0 ± 3.7	66.3 ± 2.7	34.1 ± 4.7	24.8 ± 1.1	13.9 ± 5.9
Z13	50.0 ± 2.7	43.3 ± 1.6	12.8 ± 0.9	58.6 ± 3.7	36.5 ± 3.1	37.3 ± 2.8	55.0 ± 2.4	30.6 ± 3.9	12.8 ± 0.9	10.7 ± 3.2
Z14	20.4 ± 1.3	32.7 ± 1.2	7.9 ± 3.8	57.7 ± 1.7	29.2 ± 3.5	54.1 ± 3.4	58.8 ± 3.1	29.3 ± 1.2	7.9 ± 3.8	1.2 ± 2.2
Z15	40.4 ± 3.7	53.9 ± 1.6	16.1 ± 3.2	51.5 ± 1.8	39.5 ± 2.4	45.1 ± 1.2	63.8 ± 4.2	43.1 ± 2.0	16.1 ± 3.2	19.8 ± 3.7
Z16	30.9 ± 2.8	50.6 ± 4.2	14.0 ± 1.1	47.3 ± 1.4	35.6 ± 3.2	28.8 ± 2.4	62.1 ± 3.3	45.3 ± 0.9	14.0 ± 1.1	21.0 ± 4.7
Z17	94.3 ± 0.9	83.3 ± 2.1	58.7 ± 2.3	80.3 ± 1.7	69.5 ± 3.7	66.5 ± 1.4	75.8 ± 2.3	69.0 ± 0.0	56.2 ± 3.0	53.6 ± 2.2
Z18	19.1 ± 1.5	16.7 ± 1.4	61.2 ± 3.3	53.6 ± 3.9	37.3 ± 4.0	36.5 ± 7.7	43.8 ± 3.1	72.0 ± 1.7	61.2 ± 3.3	7.1 ± 3.6
Z19	78.7 ± 1.7	61.2 ± 4.7	25.2 ± 3.2	54.0 ± 3.4	47.6 ± 4.0	54.9 ± 1.2	58.8 ± 1.9	44.0 ± 1.9	25.2 ± 3.2	27.0 ± 2.6
YMr.	40.4 ± 0.1	29.0 ± 2.1	24.4 ± 1.8	26.2 ± 1.9	33.0 ± 3.2	29.2 ± 1.9	43.8 ± 1.2	7.4 ± 2.4	33.9 ± 1.8	17.1 ± 5.9
Az[b]	65.2 ± 2.4	62.4 ± 1.1	66.1 ± 1.1	74.5 ± 1.7	60.9 ± 2.2	71.2 ± 0.9	68.8 ± 2.7	59.5 ± 1.2	66.1 ± 1.1	51.2 ± 1.8
Fl [b]	51.9 ± 1.6	–	–	–	–	–	–	–	–	–

[a] Average of three replicates, [b] The commercial antifungal agent Azoxystrobin. (Az) and Fluopyram (Fl).

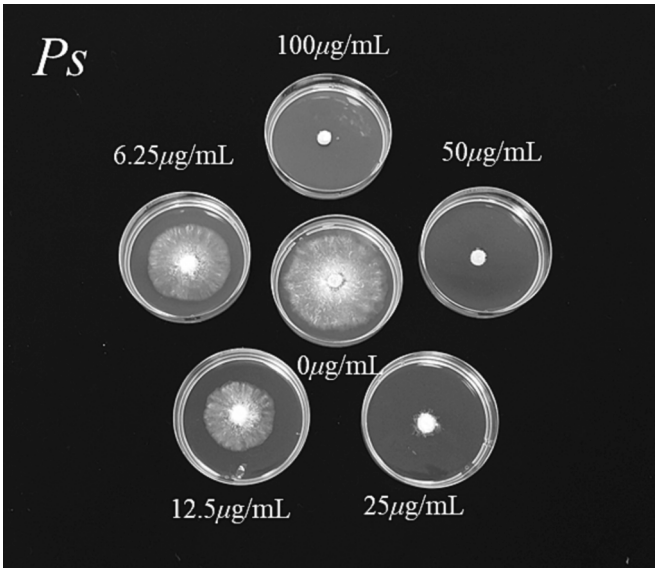

Fig. 4. *In vitro* antifungal effects of **Z17** against *Phomopsis sp* at different concentrations.

kiwifruit, superior to that of the azoxystrobin 40.7 %. The curative effect of **Z17** (31.4 %) was close to that of azoxystrobin (31.1 %). Therefore, we can draw the following conclusion that **Z17** could reduce the diameter of the lesion significantly, thereby inhibiting *Phomopsis sp* growth and exhibiting good *in vivo* antifungal activity. As shown in Fig. 5, **Z17** showed no obvious toxicity to kiwifruit at a high concentration.

3.4. *Z18 in vivo fungicidal activities resist A. brassicae*

According to Fig. 6 and Table 4, it was observed that the negative control produced a large number of spot lesions and leaf necrosis and wilt, while the leaves treated with **Z18** only formed a small number of scattered spot lesions regardless of curative or protective, and the number of spots was less than that of the control drug azoxystrobin. At

Table 2
EC_{50} values of some of the target compounds against fungi.

Compounds	Phytopathogen	Regression equation	r	EC_{50}(μg/mL)[a]
Z6	*Ss*	y = 2.6288x + 0.9667	0.9569	34.2
Z17	*Ss*	y = 1.4578x + 3.0769	0.9732	20.9
Az	*Ss*	y = 0.8128x + 3.7499	0.9812	34.5
Z6	*Ps*	y = 1.5401x + 3.3079	0.9960	12.6
Z8	*Ps*	y = 1.6356x + 2.4724	0.9836	35.1
Z17	*Ps*	y = 1.8964x + 2.9318	0.9857	12.3
Z19	*Ps*	y = 1.0323x + 3.5524	0.9347	25.3
Az	*Ps*	y = 0.6440x + 4.0290	0.9903	32.2
Fl	*Ps*	y = 1.5210x + 2.1242	0.9808	77.7
Z4	*Pc*	y = 1.1789x + 3.2549	0.9923	30.2
Az	*Pc*	y = 0.7478x + 3.8068	0.9809	39.4
Z17	*Rs*	y = 2.1291x + 1.6775	0.9853	36.4
Az	*Rs*	y = 0.5320x + 4.7451	0.9936	3.0
Z17	*Fg*	y = 1.2113x + 3.0195	0.9918	43.2
Az	*Fg*	y = 0.5534x + 4.4612	0.9986	9.4
Z17	*Bc*	y = 1.6081x + 2.2809	0.9708	49.1
Az	*Bc*	y = 1.2816x + 2.7232	0.9987	59.8
Z17	*Ab*	y = 1.9509x + 1.7919	0.9833	44.1
Z18	*Ab*	y = 1.7018x + 2.4278	0.9829	32.5
Az	*Ab*	y = 0.3965x + 4.3289	0.9853	49.3

[a] Average of three replicates.

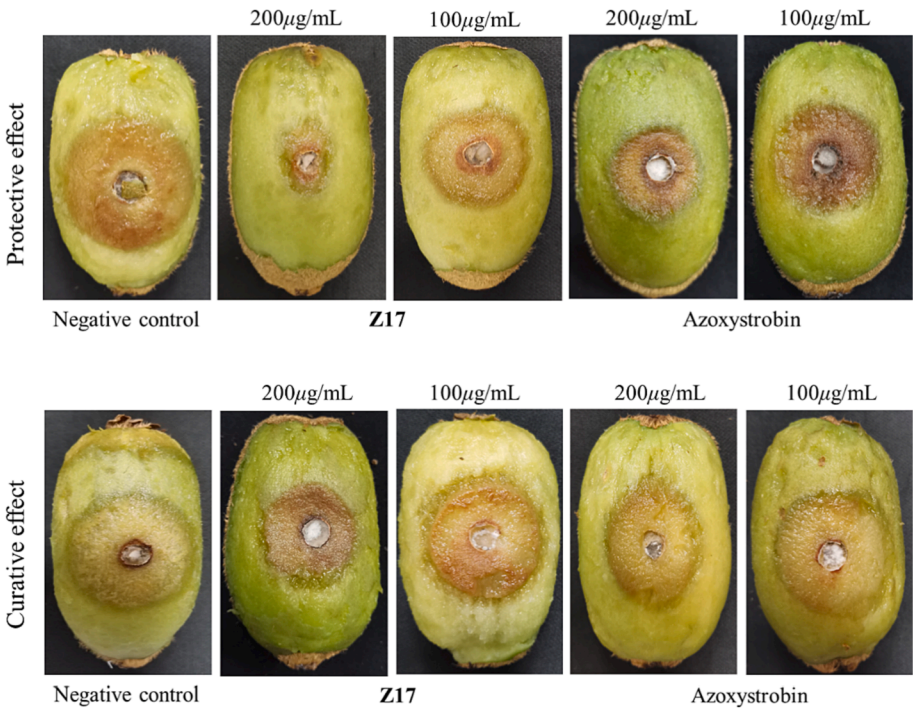

Fig. 5. The protective and curative effect of **Z17** and azoxystrobin against *Phomopsis sp* on kiwifruit.

Table 3
Curative and protective activities of **Z17** against *Phomopsis sp in vivo*.

Compound	Concentrations (μg/mL)	**Curative effect**		**Protective effect**	
		Lesion length (mm ± SD)	Control effeicacy (%)[a]	Lesion length (mm ± SD)	Control effeicacy (%)[a]
Z17	200	28.6 ± 0.5	31.4	16.2 ± 0.7	62.5
	100	35.5 ± 0.9	14.8	28.2 ± 0.8	35.7
Az	200	28.7 ± 0.4	31.1	25.6 ± 1.0	40.7
	100	36.0 ± 0.0	13.6	35.3 ± 0.5	18.3
Control	0	41.7 ± 0.8	–	43.2 ± 0.9	–

[a] Average of three replicates.

200 μg/mL, the protective and curative effects of **Z18** against *A. brassicae* on cabbage were 84.4, 81.9 %, which were superior to that of azoxystrobin 57.9, 43.5 %. In conclusion, **Z18** exhibits excellent protective and curative activities against *A. brassicae*.

3.5. Observations on the morphology of Phomopsis sp

3.5.1. Scanning electron microscope (SEM) experiment of *Z17*

The mechanism of **Z17** on *Phomopsis sp* was further studied by using SEM, which is consistent with the previous experimental conclusions. The mycelia morphology of *Phomopsis sp* treated with **Z17** changed significantly. As shown in Fig. 7, the mycelium of **group A** without drug treatment was smooth and full in morphology, good in extension and uniform in thickness. When **Z17** was 50 μg/mL (**group B**), the mycelium began to flatten, the surface was depressed, and the growth was obviously inhibited. When the concentration of the compound increased to 100 μg/mL (**group C**), the surface damage of the mycelium was aggravated, severe atrophy occurred, and the morphological folds were shriveled. In conclusion, with the increase of compound concentration, the degree of damage to mycelia intensified, which indicated that **Z17** could destroy the mycelia morphology of *Phomopsis sp* and inhibit its normal growth.

3.5.2. Fluorescence microscope (FM) imaging experiment of *Z17*

The Fig. 8 showed the situation of **Z17** treated with *Phomopsis sp* at 0, 50, 100 μg/mL and stained with PI. As can be seen from Fig. 8 **- A** and **A1**, untreated (0 μg/mL) mycelium was thin and could not be stained by PI. When **Z17** was 50 and 100 μg/mL (Fig. 8 **- B** and **B1**, **C and C1**), the mycelia had a strong shape, uneven surface, emitted strong red fluorescence obviously, and the fluorescence became stronger and stronger with the increase of drug concentration. In short, **Z17** could damage the integrity of mycelial cell membranes and have a strong impact on mycelial morphology.

3.6. Inhibition effect of *Z17* on the formation of sclerotia of Phomopsis sp

As shown in Fig. 9 and Table 5, **Z17** had a certain inhibitory effect on the formation of *Phomopsis sp* sclerotia. At a concentration of 100 μg/mL, the inhibition rate of **Z17** reached 98.0 %, which was better than that of azoxystrobin (96.5 %). It can be seen that the number of sclerotia was almost completely inhibited. And when the concentration was 50 μg/mL, a small amount of sclerotium was produced. With the reduction of the concentration of the drug, the number of sclerotia increased, but both were better than the commercial drug azoxystrobin. This indicated that **Z17** had a good effect on inhibiting the formation of *Phomopsis sp* sclerotia.

3.7. Effect of *Z17* on the cell membrane permeability of Phomopsis sp

Cell membranes are important for maintaining the integrity of cell structures and normal life activities. As shown in Fig. 10, compared with the blank control group, the relative conductivity of the mycelium increased with time after being treated with **Z17**. And when the concentration of **Z17** was at 25, 50, 100 μg/mL, the relative conductivity also increased gradually. In particular, when **Z17** was 50 and 100 μg/mL, the rising trend was more evident and increased in a concentration

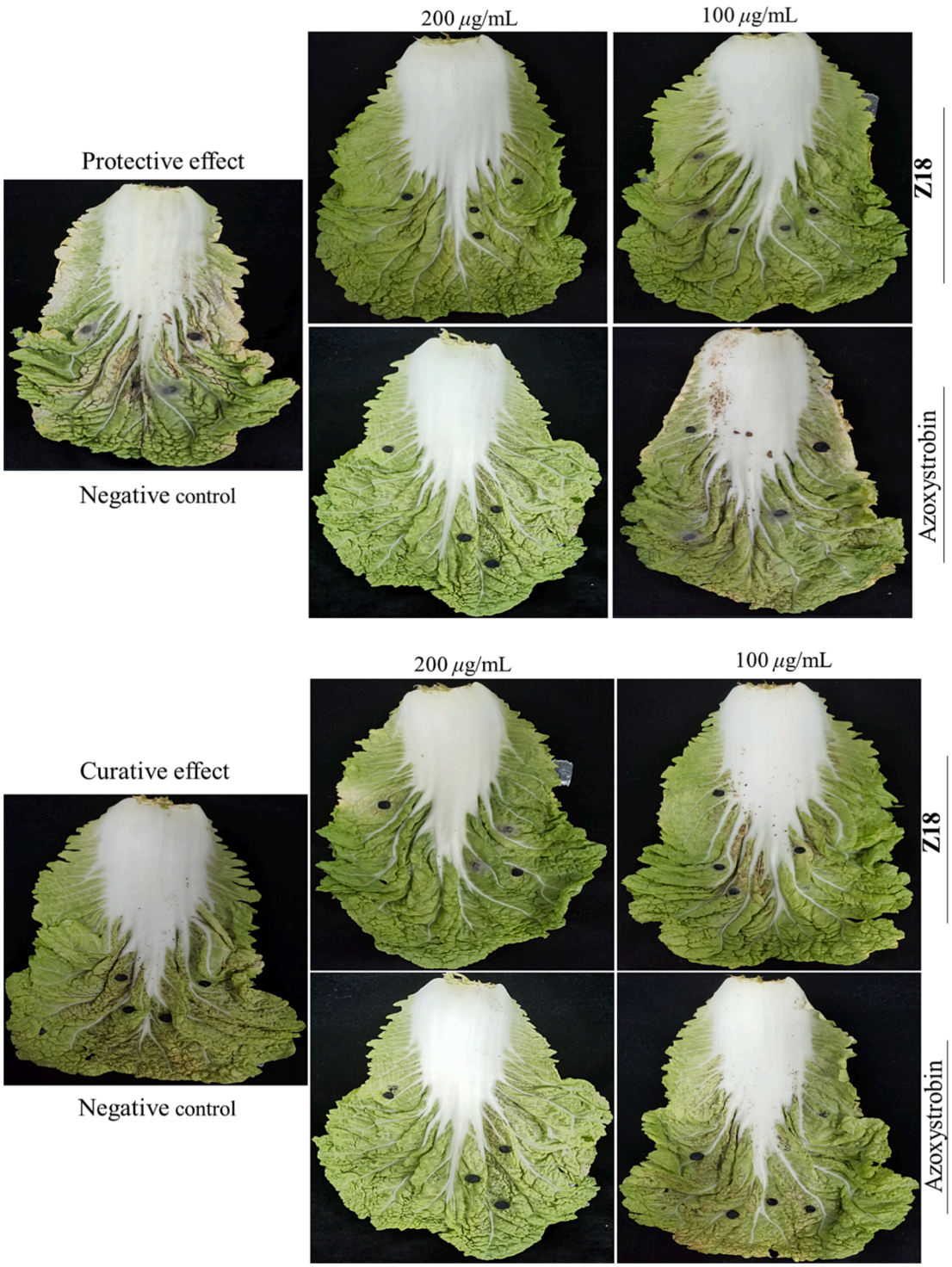

Fig. 6. The protective and curative effect of **Z18** and azoxystrobin against *A. brassicae* on cabbage.

gradient. In conclusion, **Z17** could change permeability of cell membrane and promote cell death of *Phomopsis sp*.

3.8. Effect of *Z17* on the cytoplasmic leakage of Phomopsis sp

As can be seen from the Fig. 11, the absorbance value of the **Z17** treatment group was significantly higher than that of the blank control. Especially, when the concentration was 50 μg/mL, the permeability of cytoplasmic contents increased significantly. Therefore, we could speculate that **Z17** could destroy cell membrane structure of the mycelia, thereby promote the release of intracellular contents. It was consistent with the results of SEM.

3.9. Determination of MDA content by *Z17*

The results of **Z17** on the content of MDA was shown in Fig. 12. Compared with the control group (0 μg/mL), the content of MDA in the mycelia treated with different concentrations of **Z17** (12.5, 25, 50, 100 μg/mL) increased significantly with the increase of concentration, which suggested that **Z17** can seriously damage the cell membrane of

Table 4
Curative and protective activities of **Z18** against *A. brassicae in vivo.*

Compound	Concentrations (μg/mL)	Curative effect		Protective effect	
		Lesion length (mm ± SD)	Control effeicacy (%)[a]	Lesion length (mm ± SD)	Control effeicacy (%)[a]
Z18	200	1.8 ± 0.5	81.9	1.7 ± 0.0	84.4
	100	6.3 ± 0.4	36.9	4.7 ± 0.4	56.6
Az	200	5.6 ± 0.5	43.5	4.6 ± 0.3	57.9
	100	7.3 ± 0.1	26.5	7.1 ± 0.1	35.3
Control	0	10.0 ± 0.5	–	11.0 ± 0.4	–

[a] Average of three replicates.

Phomopsis sp, and the damage degree was proportional to the concentration of the compound.

3.10. Molecular docking of *Z17* with SDH

The molecular docking simulation results indicated that **Z17** and fluopyram (SDHI) dock into the active protein pocket of SDH in a similar mode of action. As shown in Fig. 13 **A-a**, **Z17** and SDH active protein had a strong hydrogen bond interaction between the amide bond and the key amino acid residue LEU 63, and the distance between the amide bond and LEU 63 was 1.45 Å. In addition, amino acid residues PRO 64 (2.54 Å) and LEU 62 (2.67 Å) interacted with the piperazine ring and methoxy group of **Z17** through conventional hydrogen bonding. LEU 61 (2.2 Å) forms Pi-Sigma bonds with aromatic rings. PHE 86 (5.86 Å) and TYR 85 (5.44 Å, 5.82 Å) bind with S element and benzene ring through Pi-Sulfur and Pi-Pi T-shaped bonds. ALA 60 (4.12, 4.41 Å) formed Alkyl interactions and Pi-Alkyl hydrophobic with thiazole ring and *tert*-butyl groups. In Fig. 13 **B-b**, fluopyram was connected to amino acid residues VAL 53 (2.55 Å) and GLY 52 (2.70 Å) by a conventional hydrocarbon bond. And PHE 56(3.66 Å) formed the Pi-Pi Stacked interaction. LEU 83 (5.42 Å), ILE 93(4.75 Å), LEU 91(4.83 Å), LEU 55(5.21 Å) form Alkyl interactions and Pi-Alkyl hydrophobics. In summary, **Z17** formed multiple interactions with the amino acid residues of SDH, making it tightly bound to SDH. Meanwhile, the binding energy of **Z17** was −89.3 kcal mol^{-1}, which was slightly higher than that of flupyram (-−51.9 kcal mol^{-1}). It was further proved that SDH may be one of the action sites of **Z17**. These results suggested that **Z17** may destroy the mitochondrial tricarboxylic acid cycle, thus leading to the death of pathogens.

4. Conclusions

19 myricetin derivatives containing thiazole were designed and synthesized. The antifungal activity test results indicated that **Z17** and **Z18** had good inhibitory activities. The EC_{50} value of **Z17** against

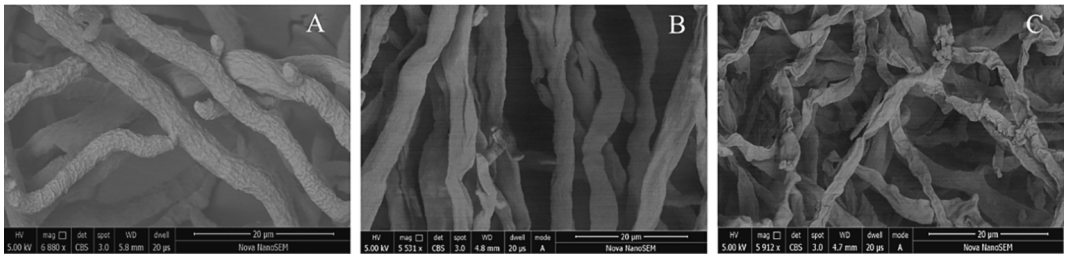

Fig. 7. SEM images of the hyphae of *Phomopsis sp* after treatment with **Z17**. (A) 0 μg/mL, (B) 50 μg/mL, (C) 100 μg/mL. Scale bar for (A-C) are 20 μm.

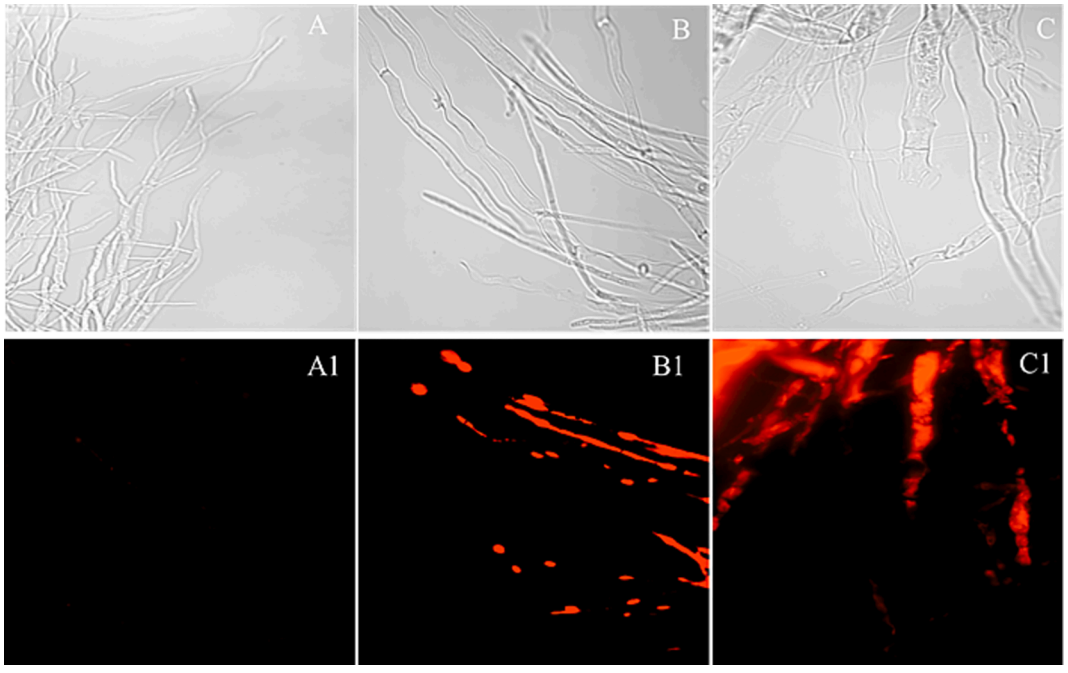

Fig. 8. Morphological observation by FM of *Phomopsis sp* treated with **Z17**. (**A-A1**) 0 μg/mL, (**B-B1**) 50 μg/mL, (**C-C1**) 100 μg/mL.

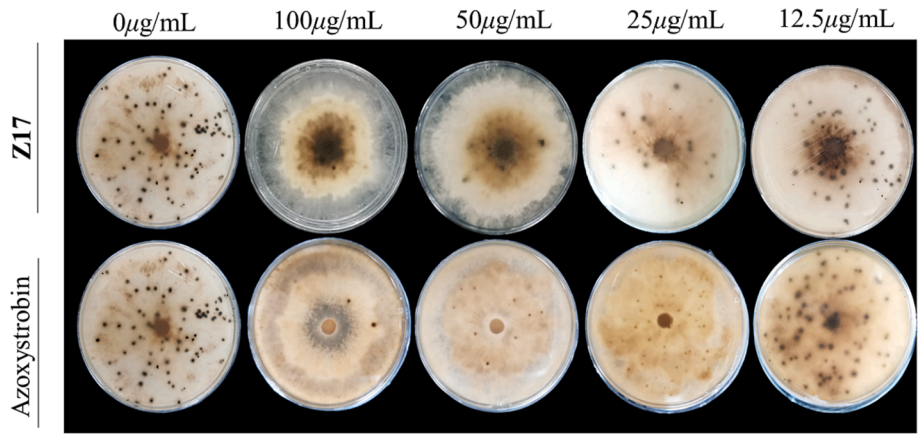

Fig. 9. The inhibitory effect of **Z17** on the formation of sclerotia of *Phomopsis sp.*

Table 5
Inhibition rate of **Z17** on *Phomopsis sp* sclerotia formation.

Compound	Concentrations (μg/mL)	Number of sclerotia	Inhibition ration (%)[a]
Z17	12.5	57.3 ± 1.3	14.4
	25.0	20.0 ± 0.7	70.1
	50.0	8.3 ± 0.5	87.6
	100.0	1.3 ± 0.5	98.0
Az	12.5	67.0 ± 2.1	–
	25.0	49.0 ± 0.8	26.9
	50.0	10.0 ± 0.6	85.1
	100.0	2.3 ± 0.6	96.5
Control	0.0	67.0 ± 0.8	–

[a] Average of three replicates.

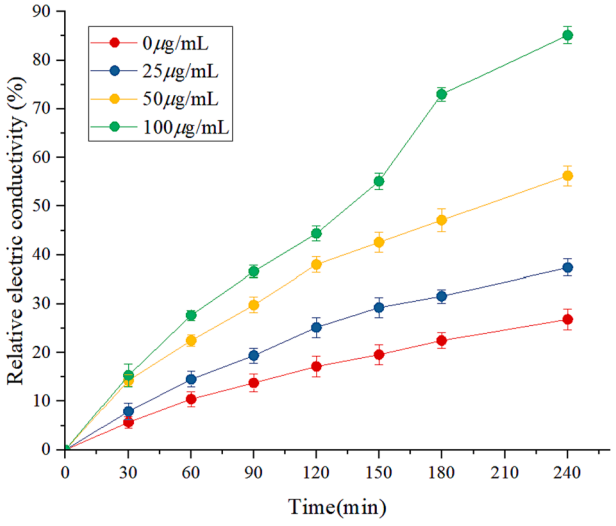

Fig. 10. Changes in cell membrane permeability of **Z17** against *Phomopsis sp.*

Phomopsis sp was 12.3 μg/mL, which was superior to those of the control drug azoxystrobin (32.2 μg/mL) and fluopyram (77.7 μg/mL). The *in vivo* experiment results indicated that **Z17** had the good protective activity against *Phomopsis sp* (62.5 %) on kiwifruit, which was better than that of azoxystrobin (40.7 %) at 200 μg/mL. **Z18** possessed an excellent protective and curative activity against *A. brassicae* (84.4, 81.9 %) on cabbage, which was superior to that of azoxystrobin (57.9, 43.5 %) at 200 μg/mL. The mechanism studies, such as molecular docking, SEM, FM, sclerotium formation, cell membrane permeability, cell content release, and MDA content were all consistent with the preliminary

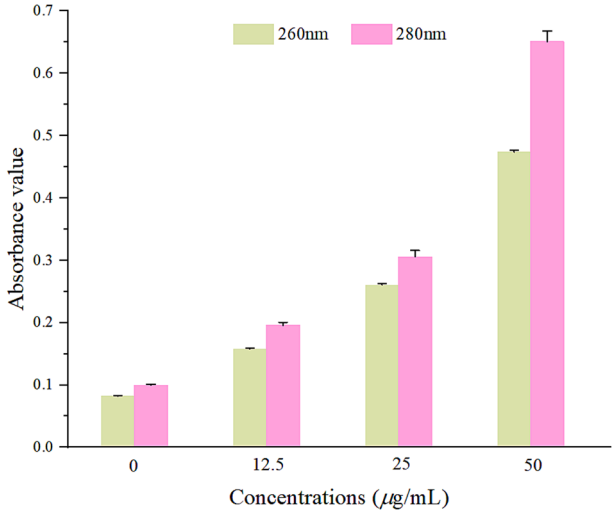

Fig. 11. Release of cellular contents from *Phomopsis sp* after treatment with **Z17.**

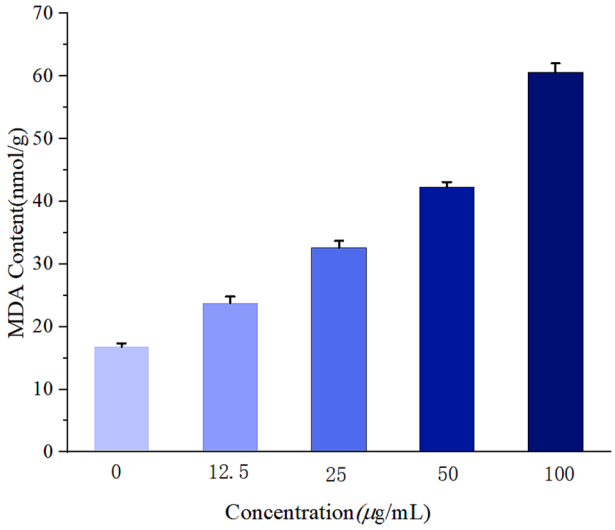

Fig. 12. MDA content of *Phomopsis sp* after treatment with **Z17.**

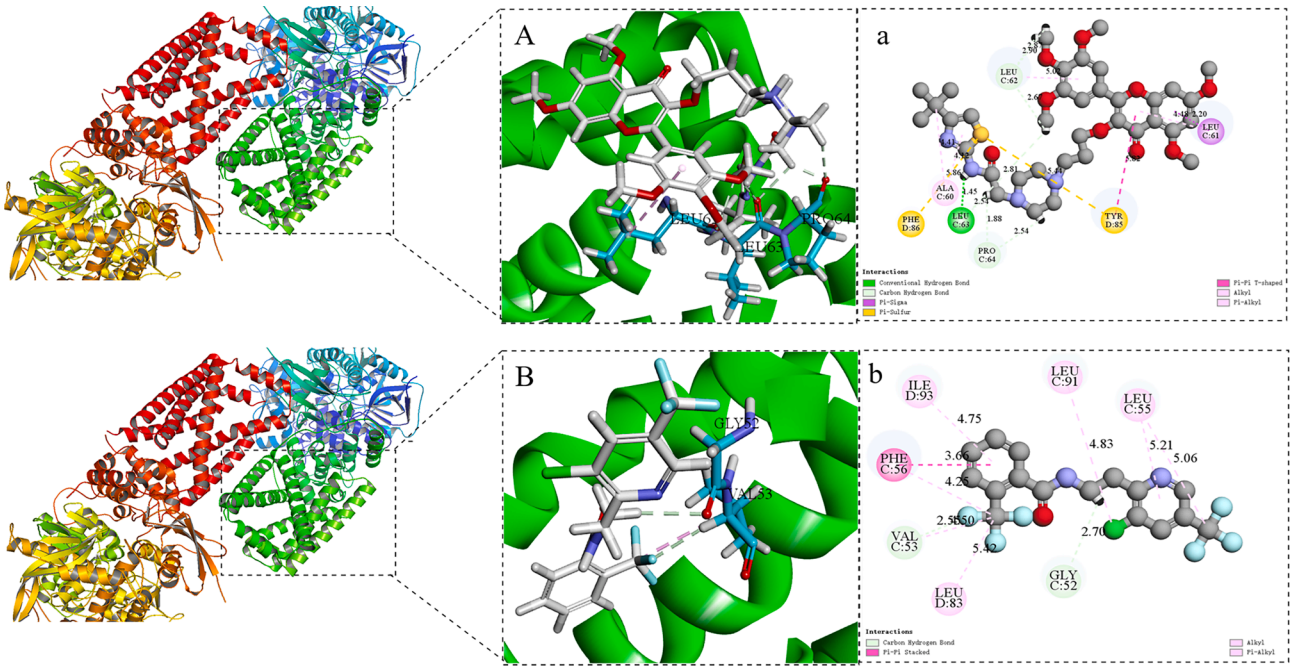

Fig. 13. Molecular docking modes of **Z17** (A-a) and fluopyram (B-b) with SDH.

screening results, which further indicated that **Z17** possessed the excellent antifungal activity. In view of this, we could affirm that **Z17** exhibited excellent antifungal activity, which also confirmed that the myricetin derivatives containing thiazole can be further developed as potential fungicides. As a result, the current work provides a new research direction and some theoretical basis for the creation of green pesticides.

Declaration of competing interest

The authors declare that they have no known competing financial interests or personal relationships that could have appeared to influence the work reported in this paper.

Acknowledgements

This research was completed with the support of the National Natural Science Foundation of China (No. 21867003), the Science Foundation of Guizhou Province (No. 20192452).

Appendix A. Supplementary data

Supplementary data to this article can be found online at https://doi.org/10.1016/j.arabjc.2023.105480.

References

Belmas, E., et al., 2018. Genome sequence of the necrotrophic plant pathogen alternaria brassicicola abra43. Genome Announc. 6 e01559-17.
Bolf, E.L., et al., 2023. Dasatinib and trametinib promote anti-tumor metabolic activity. Cells 12, 1374–1383.
Borcea, A.M., et al., 2021. An overview of the synthesis and antimicrobial, antiprotozoal, and antitumor activity of thiazole and bisthiazole derivatives. Molecules 26, 624–649.
Borelli, C., et al., 2008. Modes of action of the new arylguanidine abafungin beyond interference with ergosterol biosynthesis and *in vitro* activity against medically important fungi. Chemotherapy 54, 245–259.
Cai, W.X., et al., 2016. Synthesis and anticancer activity of novel thiazole-5-carboxamide derivatives. Appl. Sci. 6, 8–17.
Cao, X., et al., 2023. Design, synthesis and bioactivity of myricetin derivatives for control of fungal disease and tobacco mosaic virus disease. RSC Adv. 13, 6459–6465.
Chen, Y., et al., 2019. Synthesis and antibacterial and antiviral activities of myricetin derivatives containing a 1,2,4-triazole schiff base. RSC Adv. 9, 23045–23052.
Chen, S., et al., 2023. Design, synthesis and biological activity of chalcone derivatives containing pyridazine. Arab. J. Chem. 16, 1–11.
Das, J., et al., 2006. 2-aminothiazole as a novel kinase inhibitor template. structure-activity relationship studies toward the discovery of *N*-(2-chloro-6-methylphenyl)-2-[[6-[4-(2-hydroxyethyl)-1-piperazinyl)]-2-methyl-4-pyrimidinyl] amino)]-1,3-thiazole-5-carboxamide (Dasatinib, BMS-354825) as a potent pan-src kinase inhibitor. J. Med. Chem. 49, 6819–6832.
Dey, S., et al., 2016. Identification and agro-morphological characterization of rice genotypes resistant to sheath blight. Australas Plant Pathol. 45, 145–153.
Fang, H.B., et al., 2022. Discovery of arylox, arylthio, and arylamino containing acethydrazides as fungicidal agents. J. Agric. Food Chem. 71, 920–933.
Ferreira-Junior, D.F., et al., 2018. Effects of a thiamethoxam-based insecticide on the life history of chironomus xanthus. Water, Air, Soil Pollut. 229, 376–384.
Figiel-Kroczyńska, M., et al., 2021. Actinidia (mini kiwi) fruit quality in relation to summer cutting. Agronomy 11, 964–978.
Gao, F.T., et al., 2023. Synthesis and antifungal activity of curcumol derivatives. Chem. Biodiversity. 20, e202300442.
He, J., et al., 2020. Synthesis and antibacterial activity of novel myricetin derivatives containing sulfonylpiperazine. Chem. Pap. 75, 1021–1027.
He, J., et al., 2021. Discovery of zeylenone from uvaria grandiflora as a potential botanical fungicide. Pest Manage. Sci. 77, 5407–5417.
Hu, L.F., et al., 2023. Venturicidin A is a potential fungicide for controlling fusarium head blight by affecting deoxynivalenol biosynthesis, toxisome formation, and mitochondrial structure. J. Agric. Food Chem. 71, 12440–12451.
Jiang, S.C., et al., 2020. Antibacterial activities of novel dithiocarbamate-containing 4*H*-chromen-4-one derivatives. J. Agric. Food Chem. 68, 5641–5647.
Kamat, V., et al., 2020. Pyridine and thiazole-based hydrazides with promising anti-inflammatory and antimicrobial activities along with their in silico studies. ACS Omega. 5, 25228–25239.
Kanagasabapathy, G., et al., 2023. Synthesis, characterization and molecular docking studies of highly functionalized and biologically active derivatives of 2-aminothiazole. J. Mol. Struct. 1275, 134593.
Liu, T.T., et al., 2021. Design, synthesis, antibacterial activity, antiviral activity, and mechanism of myricetin derivatives containing a quinazolinone moiety. ACS Omega. 6, 30826–30833.
Liu, J., et al., 2022. Analysis of tissue-specific defense responses to *sclerotinia sclerotiorum* in brassica napus. Plants 11, 2001–2015.
Liu, F., et al., 2023. Synthesis and biological activity of myricetin derivatives containing pyrazole piperazine amide. Int. J. Mol. Sci. 24, 10442–10457.
Meng, F., et al., 2022. Design, synthesis, and antifungal activity of flavonoid derivatives containing thiazole moiety. Chem. Pap. 77, 877–885.
Ong, K.C., Khoo, H.E., 1997. Biological effects of myricetin. Gen. Pharmacol. 29, 121–126.
Peng, F., et al., 2021. Antibacterial and antiviral activities of 1,3,4-oxadiazole thioether 4*H*-chromen-4-one derivatives. J. Agric. Food Chem. 69, 11085–11094.
Peng, X.J., et al., 2023. Design, synthesis, and fungicidal activities of novel piperazine thiazole derivatives containing oxime ether or oxime ester moieties. Pest Manage. Sci. 79, 1977–1986.
Rashed, K., et al., 2014. Antibacterial and antifungal activities of methanol extract and phenolic compounds from diospyros virginiana L. Ind. Crops Prod. 59, 210–215.

Rouf, A., Tanyeli, C., 2015. Bioactive thiazole and benzothiazole derivatives. Eur. J. Med. Chem. 97, 911–927.
Silva, V., et al., 2020. Isothiazolinone biocides: chemistry, biological, and toxicity profiles. Molecules 25, 991–1012.
Tang, X., et al., 2020. Synthesis and antiviral activity of novel myricetin derivatives containing ferulic acid amide scaffolds. New J. Chem. 44, 2374–2379.
Wang, W., et al., 2020. Bioactivity-guided synthesis accelerates the discovery of 3-(Iso) quinolinyl-4-chromenones as potent fungicide candidates. J. Agric. Food Chem. 69, 491–500.
Xie, D.W., et al., 2022. Synthesis and bioactivity evaluation of 5-trifluoromethyl-1*H*-pyrazole-4-carboxamide derivatives as potential anticancer and antifungal agents. J. Heterocycl. Chem. 59, 1759–1767.
Xue, W., et al., 2015. Novel myricetin derivatives: design, synthesis and anticancer activity. Eur. J. Med. Chem. 97, 155–163.
Zeng, W.J., et al., 2023. Bioactive compounds in cruciferous sprouts and microgreens and the effects of sulfur nutrition. J. Sci. Food Agric. 103, 7323–7332.
Zhang, Z.J., et al., 2018. Discovery of β-carboline oxadiazole derivatives as fungicidal agents against rice sheath blight. J. Agric. Food Chem. 66, 9598–9607.
Zhang, X.Y., et al., 2022. Controlling black spot of postharvest broccoli by meyerozyma guilliermondii and its regulation on ROS metabolism of broccoli. Biol. Control. 170, 104938.
Zhang, M.H., et al., 2023a. Synthesis, antibacterial and antifungal activity of myricetin derivatives containing piperidine and amide fragments. Pest Manage. Sci. 79, 4795–4808.
Zhang, Y.H., et al., 2023b. Discovery of *N*-phenylpropiolamide as a novel succinate dehydrogenase inhibitor scaffold with broad-spectrum antifungal activity on phytopathogenic fungi. J. Agric. Food Chem. 71, 3681–3693.
Zhou, Q., et al., 2022. Design, synthesis, and antifungal activity of novel chalcone derivatives containing a piperazine fragment. J. Agric. Food Chem. 70, 1029–1036.
Zhou, R., et al., 2023. Design, synthesis and antifungal activity of novel 1,4-pentadiene-3-one containing quinazolinone. Int. J. Mol. Sci. 24, 2599–2612.
Zhu, J.J., et al., 2021. Synthesis of novel thiazolyl hydrazine derivatives and their antifungal activity. J. Chem. 2021, 1–8.